Effect of Shear Stress Within the Spinneret on Hollow Fiber Membrane Morphology and Separation Performance

ARTICLE *in* INDUSTRIAL & ENGINEERING CHEMISTRY RESEARCH · SEPTEMBER 1998

Impact Factor: 2.59 · DOI: 10.1021/ie9802111

4 AUTHORS, INCLUDING:

Tai-Shung Chung
National University of Singapore
727 PUBLICATIONS **19,605** CITATIONS

SEE PROFILE

Madapusi P Srinivasan
RMIT University
168 PUBLICATIONS **2,651** CITATIONS

SEE PROFILE

Effect of Shear Stress within the Spinneret on Hollow Fiber Membrane Morphology and Separation Performance

Tai-Shung Chung,*,†,‡ Soo Khean Teoh,† Wayne W. Y. Lau,† and M. P. Srinivasan†

Department of Chemical Engineering, National University of Singapore, and Institute of Materials Research and Engineering, 10 Kent Ridge Crescent, Singapore 119260, Republic of Singapore

The effects of shear stress and shear experience within a spinneret during hollow fiber spinning on membrane morphology, gas separation performance, and thermal and mechanical properties have been experimentally determined. We purposely spun the hollow fibers using a wet phase inversion process and water as the external coagulant with the belief that the effect of gravity (elongational stress) on fiber formation can be significantly reduced and the orientation induced by shear stress within the spinneret can be frozen into the wet-spun fibers. In addition, we chose 80/20 NMP/H_2O as the bore fluid with a constant bore fluid to dope fluid flow rate ratio in order to minimize the complicated coupling effects of elongational stresses, uneven internal and external solvent exchange rates, and substructure resistance on fiber formation and separation performance. Asymmetric hollow fibers for gas separation were spun from a 37% poly(ether sulfone) (PES)/*N*-methyl-2-pyrrolidone (NMP) dope solution using a spinneret with a $L/\Delta D$ (die length to flow channel gap) ratio of 17.5 that is much higher than the conventional spinneret. Experimental results suggest that hollow fiber membranes spun from this large $L/\Delta D$ die with high shear have a tighter molecular packing structure and therefore a higher selectivity that surpasses the intrinsic value but a lower permeance. For example, the selectivity of H_2/N_2 for fibers spun with high shear rate is 4-fold of the PES intrinsic value (292−307 vs 73.7). Hollow fibers spun from high shear have a lower coefficient of thermal expansion (CTE) and a higher loss modulus. Most surprisingly, we are not able to identify the nodular structure that has been observed previously in the as-cast flat membranes or at the outer skin of the hollow fibers spun from the spinneret with a small $L/\Delta D$ ratio. Clearly, the fully developed high shear stress within the spinneret has altered the thermodynamics of nodular formation, and the nodules either might not exist or become too small to be detected or deform into ambiguous elliptical shape. *For the first time*, we have also observed a *threadlike inner skin structure* in high-sheared membranes. In addition, the apparent dense layer thickness for the fiber spun with low shear is the thinnest that has ever been reported in the literature for hollow fiber membranes (450 Å).

Introduction

Membranes have been recognized as effective molecular scale separating devices and have certain advantages over more traditional chemical engineering separation approaches for some applications involving gas treatment such as cryogenic distillation, absorption, and adsorption. A phase inversion process has been used to develop the first integrally skinned asymmetric cellulose acetate membranes (Loeb and Sourirajan, 1963). The methods used for the phase inversion process include dry phase, wet phase, and dry/wet phase inversion. Gas separation membranes can be prepared in the form of flat sheets or hollow fibers (Kesting and Fritzsche, 1993; Koros and Chern, 1987). However, the spinning of hollow fibers is more complex than the formation of flat sheet membranes because it involves more controlling factors, for example, the quench conditions (temperature and composition) from both the bore fluid and the external coagulant, the dimensions of the spinneret used (inner tube and orifice), the dope extrusion rate, the length of the air gap (for a dry-jet wet-spinning process), the fiber wind-up speed, and the coupling effect of the ternary system consisting of polymer, solvent and coagulant (Chung, 1997; Chung and Kafchinski, 1997; Koros and Pinnau, 1994; Puri, 1990).

In hollow fiber spinning, the pressurized viscous polymer solution will be subjected to various stresses when it extrudes through the complicated channel within a spinneret. These stresses may affect molecular orientation and relaxation, subsequently fiber formation and separation performance, and fiber productivity. *As a result, the design of spinnerets has been treated as a trade secret (know how) and very rare attention has been given in academia to study fundamentally the effects of spinneret design and fluid behavior within the spinneret on hollow fiber membrane formation*. Much of the previous work that has been published focused on other spinning parameters that occur outside the spinneret, for example, the effects of coagulant and bore fluid temperature and chemistry of internal and external coagulants on the structure and properties of hollow fiber membranes (e.g., Aptel and Cabasso, 1981; Borneman et al., 1986; Wienk et al., 1996) or on the fundamentals of mass transfer for flat membranes (Matsuura, 1994; McHugh and Miller, 1995; Chung and Teoh, 1997).

There are probably two dominant mechanisms to induce molecular orientation during the phase inversion

* To whom all correspondence should be addressed.
† National University of Singapore.
‡ Institute of Materials Research and Engineering.

S0888-5885(98)00211-5 CCC: $15.00
Published on Web 09/03/1998

of fiber formation. One is due to the elongational stresses (outside the spinneret) of gravity and spin line stresses (e.g., Paul, 1969; El-hibri and Paul, 1985; Chung, 1997). The other is due to the shear and elongational stresses within the spinneret (Aptel et al.; 1985, Shilton et al., 1994, 1996). However, the development of molecular orientation during the phase inversion is also coupling with both the internal and external demixing that affects the relaxation and thermodynamic state of molecular chains. In addition, molecules may experience die swelling and relaxation when exiting from the spinneret if there is an air gap before coagulation and thus may change its orientation immediately. Therefore, unless the experiments are well-designed, one cannot decouple shear, elongational, gravity, and coagulation effects on fiber formation.

Aptel et al. (1985) suggested that the orientation of polymer molecules induced in the spinneret would affect the properties of dry-jet wet-spun hollow fibers for ultrafiltration application. They found that increasing the dope flow rate would increase the shear stress and, in turn, reduce the permeability. However, they have kept the bore fluid rate constant while varying the dope flow rate, and thus the complicated coupling effects of bore fluid rate on fiber formation was not discounted.

East et al. (1986) have studied the effect of polymer extrusion rate on dry-jet wet-spun polysulfone hollow fiber properties and found that increasing the dope extrusion rate would reduce the gas permeation rate and increase the selectivity. However, similar to the case of Aptel et al. (1985), they did not keep the ratio of dope to bore fluid rate constant.

Recently, Shilton et al. have shown that both gas permeability and selectivity increased with an increase in the dope extrusion rate. The increase in selectivity is due to enhanced orientation in the skin of dry-jet wet-spun polysulfone hollow fibers. The increase in permeability with an increase in the dope flow rate (or molecular orientation) seems to be contradictory to that of Aptel et al. (1985) and East et al. (1986). Shilton et al. claimed that the peculiar phenomenon was related to the variation of surface porosity with various flow rates. They have also found that tensile properties of the fibers formed are *not sensitive* to the dope extrusion rate and *no distinct morphology change* is observed with regard to the shear effect (Shilton et al., 1994; 1996). However, in their work, the fibers were dry-jet wet-spun. As a result, *they have coupled both the shear and air gap (elongational stress) effects in the fiber formation and their data analysis*. In addition, since their spinning solution is a viscoelastic fluid, molecular orientation induced by shear stress within the spinneret might relax in the air gap region if the elongational stress along the spin line is small or might enhance if the spin line stress is high. Furthermore, they used water as the internal coagulant. Water is a very powerful coagulant, and it will surely result in the formation of a relatively dense inner skin. Therefore, their hollow fibers might have two relatively dense skins, and no one could be sure if the elongated inner skin structure played an important role in their fiber separation and mechanical performance.

The induced orientation by shear or elongation stresses may enhance fiber thermal and mechanical properties. For example, Yang and Chou (1996) found that the breaking strength and breaking elongation of poly(acrylonitrile) hollow fibers increased with the draw ratio for samples in the dry state. The pore size and hydraulic permeability of pure water also increased with the draw ratio. Ismail et al. (1997) used plane-polarized infrared spectroscopy to measure the molecular orientation in the active layer of a dry-jet wet-spun polysulfone hollow fiber and demonstrated that there was an increased molecular orientation in the high-sheared membrane that enhanced the gas selectivity. However, similar to the previous case of Shilton et al., the effect of air gap or elongational stress was also not discounted.

To our knowledge, a systematic study on the effects of shear stress and shear experience within a spinneret in relation to hollow fiber membrane formation, morphology, thermal and mechanical properties, and separation performance *has not* been done. Since there are shear, converging, and diverging flows within the flow channel of a spinneret, in this paper, we have designed a special spinneret to create mainly shear flow within the spinneret to define the shear stress effects on fiber membrane formation. To decouple the shear and elongational stresses applied to a fiber during its formation and to reduce the relaxation effect on molecular orientation, we have purposely spun the hollow fibers using a wet phase inversion process and used water as the external coagulant with the belief that the effect of gravity (elongational stress) on fiber formation can be significantly reduced and the orientation induced by shear stress within the spinneret can be frozen into the wet-spun fibers. In other words, for fibers spun with a wet phase inversion process and rapid coagulation, more of this enhanced orientation will be frozen into the solidified polymer when the polymer solution emerges from the spinneret and phase-separated in the external coagulant bath because the coagulation time is probably shorter than the relaxation time of this viscoelastic fluid. In addition, we used 80/20 NMP/H_2O as the internal coagulant in this work to ensure that there is only one selective skin, and therefore the substructure effect on separation performance and data analysis is minimized.

To characterize membranes made from different shear stress experiences, we also investigate the dynamic mechanical and thermomechanical properties over a wide range of temperatures and frequencies in this work.

Experiments

Poly(ether sulfone) (PES) Radel A-300 was purchased from Amoco Performance Products Inc., OH, USA. It has a weight-average molecular weight of about 15 000. The solvent used, *N*-methyl-2-pyrrolidone (NMP, >99%) was supplied by Merck. *The NMP was chosen as the solvent because its density is about 1.03 g/cm^3 which is almost the same as water; as a result, we may reduce the effect of buoyancy*. Other organic solvents are reagent grade and used as received. PES powder was dried in the oven for approximately 3 h at about 120 °C to remove its moisture content. Then, 37% of PES powder was dispersed slowly into 63% of a chilled NMP solvent (0−3 °C, contained in a flask that was immersed in an ice bath) and stirred continuously with a high-speed mechanical stirrer at room temperature. The chilled solvent will reduce the dissolvation rate of PES powder and consequently prevent the powder from agglomeration at the initial stage of stirring (Chung and Kafchinski, 1997). The viscosity of the polymer solution as a function of shear rate was determined from a Ares Rheometric Scientific rheometer with a 25 mm parallel

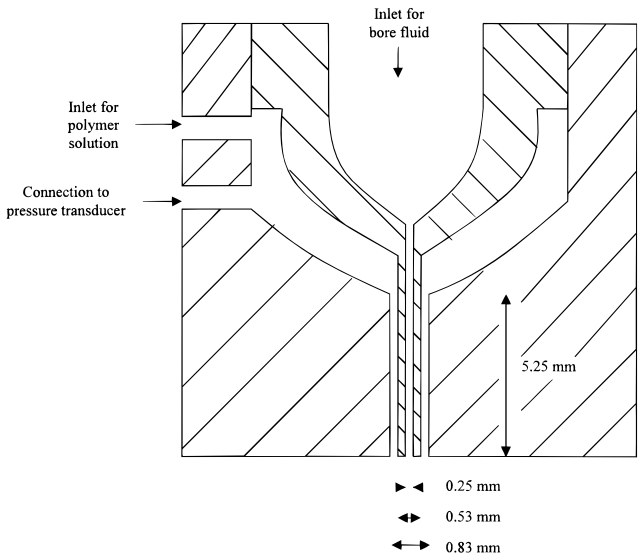

Figure 1. Schematic diagram of the spinneret for hollow fiber spinning. L/D ratio = 17.5.

plate. These rheological data provided a relationship between shear stress τ (in N/m^2) and shear rate $\dot{\gamma}$ (in 1/s) as follows: for 37% PES/NMP dope,

$$\tau = 115.95|\dot{\gamma}|^{0.7526}$$

The shear rates and shear stresses experienced at the external wall of the annular region in the spinneret were then estimated using the power law model (Bird et al., 1987; Fredrickson and Bird, 1958; Shilton, 1997).

Figure 1 illustrates the design and dimensions of the new spinneret. A Druck PDCR 200 pressure transducer with an accuracy of 0.1 psi was installed in the upper part of the flow channel. The o.d. and i.d. of the annular channel for the spinning solution are 830 and 530 μm, respectively. This new spinneret is different from the conventional spinnerets in terms of the $L/\Delta D$ ratio. The typical $L/\Delta D$ ratio for conventional hollow fiber spinning is within 1−5 (Tadmor and Gogos, 1979) (in order to reduce pressure drop and increase productivity), whereas ours is 17.5. Since it has been recognized that, for flow in the capillary, a L/D (D is the flow channel) ratio of greater than 10 might be necessary to provide a fully developed flow (Pearson, 1985), a large $L/\Delta D$ (ΔD is the flow channel) is chosen in this case. In addition, the $L/\Delta D$ ratio used in our case is much greater than the calculated value (Crochet et al., 1984) for development of steady shear flow for a power law fluid in the entrance region of a plane narrow channel. As a result, we are sure that a simple steady shear flow is developed in the new spinneret.

The formulated dope was fed into the annulus of the spinneret under pressurized nitrogen gas. The dope extrusion rate was altered by varying the pressure that imposed onto the polymer solution passing through the spinneret while other parameters were kept constant. The dope flow rate can independently be measured using a microbalance underneath the spinneret. Bore fluid was fed into the inner tube (i.d. = 250 μm) of the spinneret by an ISCO 500D syringe pump with an accuracy of 0.5% flow rate. Once the spinning dope and the bore fluid meet at the tip of the spinneret, they will enter the coagulation (water) bath straight away, i.e., wet-spinning. The ratio of bore flow rate to dope flow rate is maintained almost constant (0.61−0.62) in order to reduce the complicated coupling effects (dragging, uneven demixing, and others) of the bore fluid rate on fiber formation. All the nascent fibers produced were not stretched by drawing which meant the take-up velocity of the hollow fibers was almost the same as its free-falling velocity in the coagulation bath. As a result, the effects of elongational stress and gravity on fiber formation could be significantly minimized. Water is a powerful coagulant and was used as the external coagulant in order to yield an outer selective layer and to freeze the orientation induced by shear stress within the spinneret into the solidified polymer when the polymer solution emerges from the spinneret. In addition, a mixture of 80/20 (weight ratio) NMP/H_2O was employed as the internal coagulant in order to create a porous inner structure and minimize the substructure effect on fiber performance.

Table 1. Experimental Parameters for the Spinning of 37% PES/NMP Hollow Fibers

dope solution	PES/NMP
polymer concentration (wt %)	37
dope pressure (psi)	40.6, 154.2, and 200.3
bore fluid composition	80/20 NMP/H_2O
air gap distance (cm)	0 (wet spinning)
external coagulant	water
coagulant temperature (°C)	25
spinneret temperature (°C)	25
room relative humidity (%)	74

Table 1 summarizes the spinning conditions, and Table 2 shows the calculated shear rate and shear stress induced in the outer surface of hollow fibers during spinning as estimated from the power law model. The as-spun fibers were immersed in water at room temperature for at least 1 day. Subsequently, they were immersed in fresh methanol for at least 45 min to allow sufficient solvent exchange, i.e., complete removal of residual NMP, and then air-dried overnight on tissue paper at room temperature. Hollow fibers thus treated were used for further test and study.

To test the performance of these fibers in terms of permeation rate and permselectivity, four fibers around 10 cm in length were assembled into bundles to make gas modules and the procedure has been described elsewhere (Chung et al., 1998). Gas permeation rate was determined with a bubble flowmeter (for lower flow rate) and a Matheson gas flowmeter (for higher flow rate) at 25 °C. Types of gases being tested were O_2, N_2, He, and H_2. For uncoated fibers, we used 100 psi (7 bar) of N_2 and O_2 and 70 psi (5 bar) of He and H_2. For coated fibers, we used 200 psi (14 bar) of N_2 and O_2 and 100 psi of He and H_2. Experimental data indicated that, for gas H_2 and He, there is no difference in permeance found between feed pressures of 100 and 200 psi of He and H_2. The permeance is calculated with the following equation:

$$\left(\frac{P}{l}\right)_i = \frac{Q_i}{\Delta P A} = \frac{Q_i}{n\pi D l \Delta P}$$

where $(P/l)_i$ = permeance of a membrane to gas i (GPU), Q_i = volumetric flow rate of gas i at standard temperature and pressure, (cm^3/s), ΔP = trans-membrane pressure drop (cmHg), A = membrane surface area (cm^2), n = number of fibers tested, D = outer diameter of the hollow fibers, and l = effective length of the hollow fibers.

The unit of gas permeance used is GPU, where one GPU is equal to 1×10^{-6} cm^3 (STP)/cm^2·s·cmHg. The

Table 2. Dope Flow Rate, Bore Fluid Flow Rate, Fiber Take-up Rate, Shear Rate and Shear Stress Induced in the Outer Surface of Hollow Fibers during Spinning

fiber i.d.	transducer pressure (psi)	dope flow rate (cm^3/min)	bore fluid flow rate (cm^3/min)	fiber take-up rate (cm/min)	shear rate (1/s)	shear stress (N/m^2)
1	40.6	0.042	0.026	< 27	103	3806
2	154.2	0.196	0.120	61	609	14455
3	200.3	0.284	0.174	82	862	18772

Table 3. Outer Diameter, Inner Diameter, and Wall Thickness of Hollow Fibers

fiber i.d.	dope flow rate (cm^3/min)	bore fluid flow rate (cm^3/min)	o.d. (μm)	i.d. (μm)	wall thickness (μm)
1	0.042	0.026	750	433	158.5
2	0.196	0.120	783	433	175
3	0.284	0.174	808	488	160

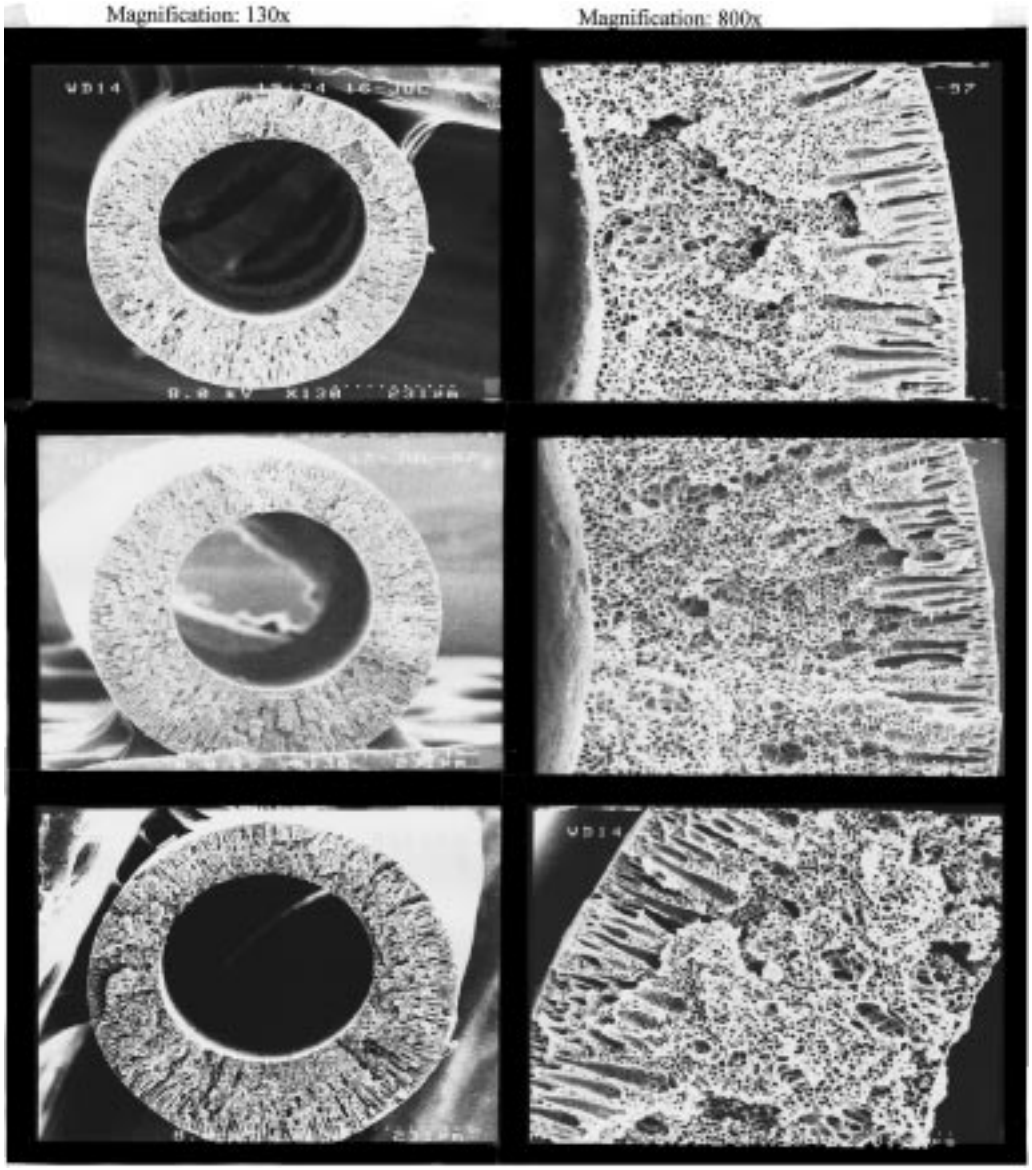

Figure 2. Cross section of hollow fibers (top, low shear (103 s^{-1}); middle, shear rate = 609 s^{-1}; bottom, high shear (862 s^{-1})).

selectivities of PES for O_2/N_2 were reported to be 6.1 with a permeability of 0.51 barrer at 30 °C and 5.1 with a permeability of 0.81 barrer at 50 °C (Wang, 1996). One may calculate permeability of O_2 at 25 °C to be about 0.44 barrer by using an Arrhenius relationship between permeability and temperature. Permeabilities of H_2 and He are 5.8 and 7.63 at 30 °C, respectively (Wang, 1996).

The ideal separation factor of an asymmetric membrane for gas A to gas B is defined as follows:

$$\alpha_{A,B} = \frac{(P/l)_A}{(P/l)_B}$$

After the uncoated fibers were tested, they were dipped into a coating solution containing 3 wt % poly(dimethylsiloxane) (Sylgard-184) in 97% *n*-hexane for 2 min to seal the membrane defects.

For SEM study, fiber samples were immersed in liquid nitrogen and fractured and sputtered with gold

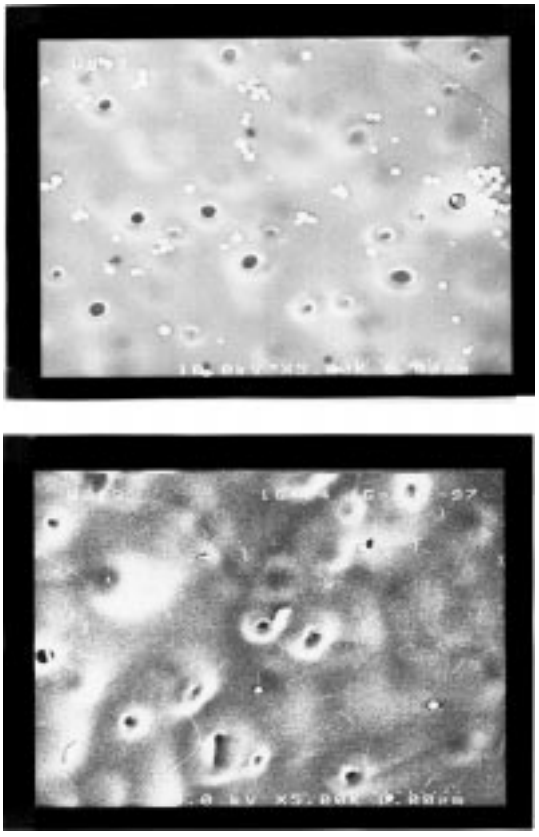

Figure 3. Inner surface of hollow fibers (top, low shear (103 s^{-1}); bottom, high shear (862 s^{-1}); magnification, ×5000).

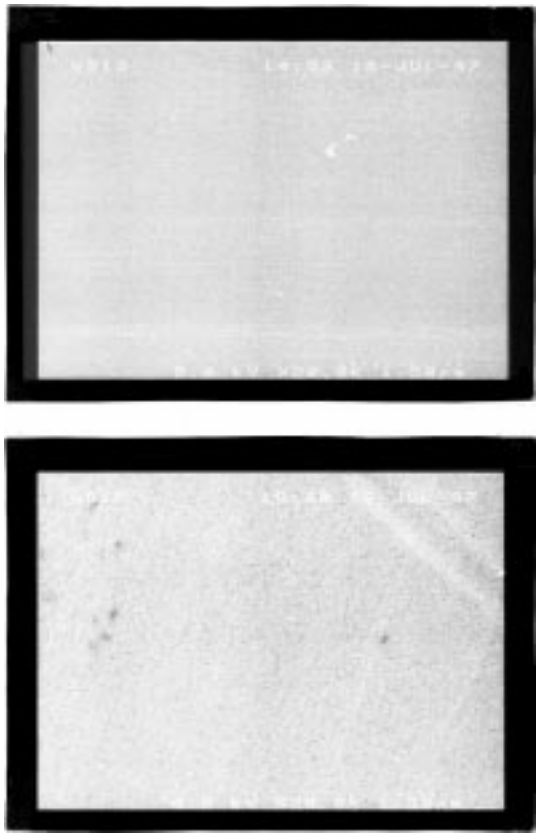

Figure 4. Outer surface of hollow fibers (top, low shear (103 s^{-1}); bottom, high shear (862 s^{-1}); magnification, ×20 000).

using a JEOL JFC-1100E ion sputtering device. To investigate the structure and morphology of the fibers, these samples were observed under a JEOL JSM U3 electron microscope and a Hitachi S-4100 field emission SEM.

CTE (coefficient of thermal expansion), loss modulus, tangent δ, and T_g were used to characterize the as-spun fibers using Thermal Instruments TMA 2940 (thermomechanical analyzer) and Thermal Instruments DMA 2980 (dynamic mechanical analyzer). When using TMA, the hollow fiber sample was heated from room temperature to 250 °C at a heating rate of 5 °C/min. The dimensional change of the hollow fiber was observed as a function of temperature. When DMA was employed, the hollow fiber sample was heated from room temperature to 250 °C at a heating rate of 3 °C/min and frequencies of 1 and 10 Hz. The dynamic modulus (stiffness) and damping (energy dissipation) of a material are measured as a function of temperature at a certain frequency as the material is deformed under periodic stress. The dynamic loss modulus or internal friction is sensitive to molecular motion, transitions, and relaxation processes of polymers (Turi, 1981; Mark et al., 1984; Murayama, 1985−1990).

Results and Discussion

1. Hollow Fiber Morphology. Table 3 summarizes the dimensions of the hollow fiber produced, and Figure 2 shows the SEM pictures of the cross section of hollow fibers spun from different shear rates but with a constant ratio of bore flow rate to dope flow rate. Since the changes in fiber dimension (o.d., i.d., and wall thickness) and cross-sectional morphology are very minor, this suggests that the internal coagulation which occurred at the lumen might be almost the same for these three cases and we may have almost achieved our objective: that is, the effects of bore fluid rate and shear stress (or shear rate) on fiber morphology have been decoupled. In addition, the o.d. of wet-spun fibers varies from 750 to 830 μm, while the o.d. of the spinneret is about 830 μm. The draw ratio (cross section of the hollow fiber product to that of the spinneret) is about 1, which again indicates that we have significantly eliminated the drawing effect of gravity on fibers.

From Figures 2 to 4, it can be seen that the inner surface of these hollow fibers is fully porous and the outer surface is dense regardless of low or high shear. These membranes were formed by an instantaneous liquid−liquid demixing process with a thin skin layer formed on top of an open-cell substructure. Since substructure plays an important role in membrane performance (Pinnau and Koros, 1991), *the morphology of this single outer dense (selective) layer confirms our objective to decouple the effect of substructure on membrane performance.*

We observed two interesting inner skin morphologies. Some dispersed polymer-rich particles were found on the inner surface of hollow fibers spun with low shear rate, while some threadlike fibers were noticed on the inner surface of the fibers spun with high shear rate. The former was due to the fact that, at the fiber inner surface, the polymer concentration was lower at this particular region, leading to the nucleation and growth of the localized polymer-rich phase that produced low-integrity polymer agglomerates. Upon completion of the slow precipitation, the resultant morphology was an interconnected open-cell structure with some dispersed polymer-rich particles attached to the inner surface. The latter was caused by the high shear where some of these

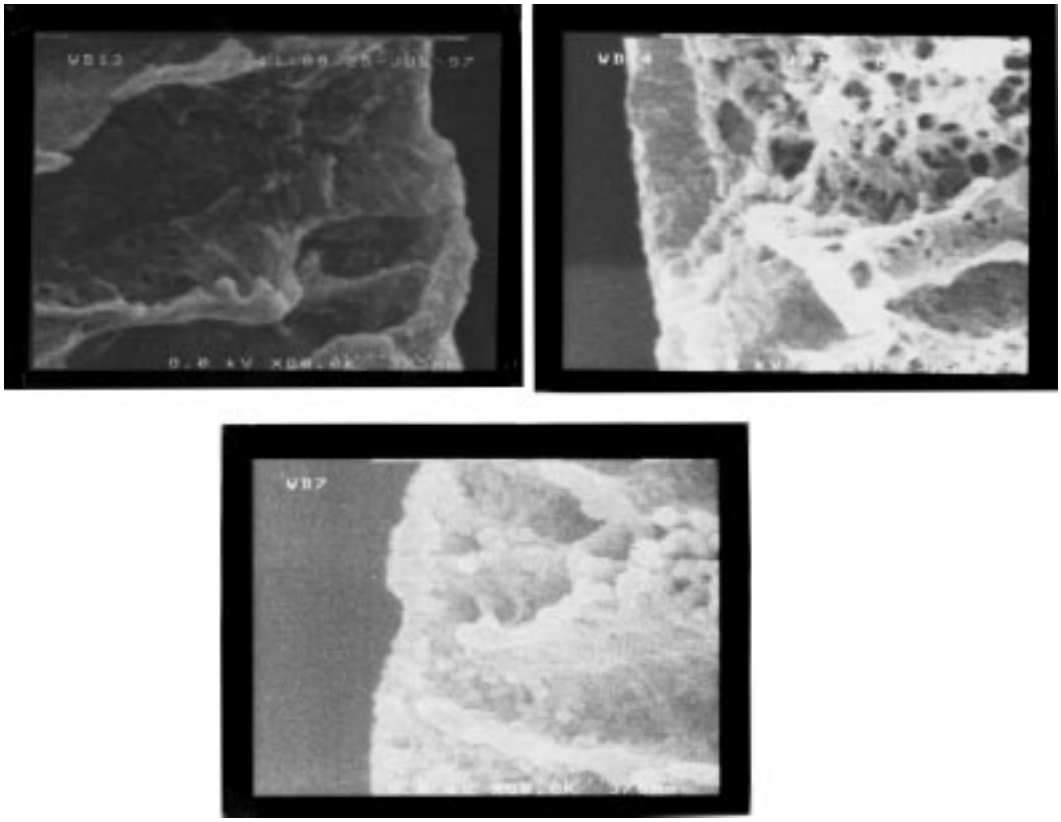

Figure 5. Outer skin of hollow fibers (top left, low shear (103 s^{-1}); top right, high shear (862 s^{-1}); bottom, 35% PES/NMP hollow fiber spun with a low *L*/*D* ratio (391 s^{-1}); magnification, ×80 000; Chung et al., 1997).

agglomerates were stretched and became threadlike fibers. This threadlike fiber structure has not been reported previously.

Since water, the powerful coagulant was used as the external coagulant, it caused the formation of a thin outer skin layer. *However, surprisingly, we are not able to identify the nodular structure (for 80 000 × magnification) that has been observed previously in the outer skin of the hollow fibers spun from 35% PES/NMP dope (Figure 5).* This phenomenon might be due to the fact that shear experience also plays an important role in membrane morphology. The $L/\Delta D$ ratio of the newly developed spinneret (for fibers spun from 37% PES/NMP dope) is 17.5, whereas the $L/\Delta D$ ratio of the previous spinneret (for fibers spun from 35% PES/NMP dope) is only 3.5 (Chung et al., 1997). Although the calculated shear rate of fibers spun from the high $L/\Delta D$ spinneret (for 37% PES/NMP with 103 s^{-1} shear rate) is lower than that of fibers spun from the low $L/\Delta D$ one (for 35% PES/NMP with 391 s^{-1} shear rate), the nodular structure is still not visible for the 37% PES/NMP hollow fiber spun with a high $L/\Delta D$ die and a low shear rate (Figure 5). This shows that the effect of a high $L/\Delta D$ ratio might be sufficiently great to distort the shape of the nodular structure rather than the shear effect alone. The dope flow in the die with a high $L/\Delta D$ ratio is fully developed, but it is not so developed in the low $L/\Delta D$ die. Nodular structure is formed in the later stages of spinodal decomposition whereby interfacial tension between polymer-rich and polymer-lean phases disrupts the bicontinuous network and promotes phase sphericity (Koros and Pinnau, 1994). Polymer molecules that undergo shear stress for a period of time will align themselves to the shear stress field. The energy balance and the state of solution will be altered (Wolf, 1984; Criado-Sancho et al., 1991, 1995; Chung and Teoh, 1997) and thus affect nodular formation. However, this work *does not rule out* the possibility of the existence of nodules in fibers spun from high shear stress because nodules might become too small to be detectable or deformed into ambiguous elliptical shape.

Table 4. Effect of Shear Rate on the Permeance of Uncoated Fiber Samples

calcd shear rate (1/s)	permeance (GPU)			
	O_2	N_2	He	H_2
103	99.3	106.0	596	1470
	112.6	120.2	642	1621
	96.0	99.0	589	1451
	97.2	100.4	570	1464
average	101.3	106.4	599	1502
609	40.3	43.0	326	784
	43.7	46.6	326	784
	34.9	37.2	308	704
	45.7	42.7	323	829
average	41.2	42.4	321	775
862	24.6	19.7	224	507
	32.0	31.1	235	564
	27.7	23.6	212	535
average	27.6	24.1	221	530

2. Separation Performance: Permeance and Permselectivity. Tables 4 and 5 clearly show that the permeances for both uncoated and coated fibers decrease with an increase in the shear rate. This can be explained by the rheological behavior of the polymeric dope as it extrudes along the annular region of the spinneret. Molecular chains that experienced higher shear tend to align themselves much better than those that experienced lower shear, and this enhanced orientation will cause the polymer molecules to pack closer to each other, leading to a lower free volume or a tighter structure. Nevertheless, this will restrict the mobility of the amorphous chain, which is necessary for the

Table 5. Effect of Shear Rate on the Permeance and the Apparent Dense Layer Thickness of Coated Fiber Samples

calcd shear rate (1/s)	permeance (GPU)				dense layer thickness calcd based on O_2 (Å)
	O_2	N_2	He	H_2	
103	9.3	1.9	241	475	
	8.8	1.6	215	409	
	9.9	2.0	244	488	
	11.4	2.0	248	475	
average	9.9	1.9	237	462	450
609	5.7	1.0	152	335	
	6.2	1.0	152	308	
	6.5	1.2	162	341	
	6.6	1.1	162	313	
average	6.3	1.1	157	324	706
862	4.9	0.8	139	282	
	4.4	0.9	124	244	
	5.6	0.9	141	243	
average	5.0	0.9	135	256	893

Table 6. Effect of Shear Rate on the Average Selectivity of Uncoated Fiber Samples

calcd shear rate (1/s)	selectivity			
	O_2/N_2	H_2/N_2	H_2/He	He/N_2
103	0.94	13.87	2.47	5.63
	0.94	13.49	2.52	5.35
	0.97	14.67	2.47	5.95
	0.97	14.58	2.57	5.68
average	0.96	14.15	2.51	5.65
609	0.94	18.23	2.41	7.57
	0.94	16.82	2.41	6.99
	0.94	18.91	2.29	8.26
	1.07	19.43	2.57	7.57
average	0.97	18.35	2.42	7.60
862	1.25	25.78	2.27	11.36
	1.03	18.14	2.40	7.57
	1.17	22.67	2.52	8.99
average	1.15	22.20	2.40	9.31

Table 7. Effect of Shear Rate on the Selectivity of Coated Fiber Samples

calcd shear rate (1/s)	selectivity			
	O_2/N_2	H_2/N_2	H_2/He	He/N_2
103	4.83	246.6	1.97	125
	5.43	252.0	1.90	133
	4.94	242.5	2.01	120
	5.84	244.0	1.91	128
average	5.26	246.3	1.95	127
609	5.99	349.8	2.20	159
	6.08	303.7	2.03	150
	5.69	296.8	2.11	140
	5.79	275.9	1.94	142
average	5.89	306.6	2.07	148
862	5.99	342.3	2.03	169
	4.97	273.7	1.97	139
	5.98	261.3	1.72	152
average	5.65	292.5	1.91	153

opening of a transient molecular scale passageway into which the gas molecule or penetrant can jump. Subsequently, the transport of gases through the free space within the polymer network will be hindered, and inevitably this will lead to a lower permeance. As a result, the apparent dense layer thickness is increased with an increase in the shear rate, as illustrated in Table 5.

From Tables 6 and 7, we observe that for most of the gas pairs studied, the permselectivities of these coated and uncoated hollow fibers show a trend of increases with increases in shear rate. For uncoated fibers with low shear (Tables 6 and 8), it can be seen that the selectivity exhibits a combination of Knudsen diffusion and solution diffusion mechanisms because for some of the gas pairs the selectivities are is higher than those predicted from the Knudsen diffusion mechanism. The high permeance of H_2 shown in Table 5 may be due to the fact that hydrogen has a linear molecule which can diffuse through the oriented outer skin faster than the spherical molecules of He.

Table 8. Selectivity of Uncoated Hollow Fibers Exhibiting the Knudsen Diffusion Mechanism

	gas pair			
	O_2/N_2	H_2/N_2	H_2/He	He/N_2
α	0.94	3.74	1.41	2.65

Table 9. Comparison of Gas Selectivity between Our Coated Hollow Fibers and Dense Films

shear rate (1/s)	O_2/N_2	H_2/N_2	H_2/He	He/N_2
103	5.26	246	1.95	127
609	5.89	307	2.07	148
862	5.65	293	1.91	153
dense film[a]	6.29[a]	73.71[a]	0.79[a]	93.57[a]

[a] Data at 25 °C and 10 bar (Wang, 1996).

However, for high-sheared uncoated fibers, the selectivities of all the gas pairs studied are contributed solely to the solution diffusion mechanism because all the gas selectivities observed are higher than those calculated from the inverse square root ratio of the molecular weights of the desired gas component to the undesired gas component. Solution diffusion separation is based on both the solubility and mobility of the penetrants in which the thermally agitated motion of chain segments generates penetrant-scale transient gaps that enable the sorbed penetrants to diffuse across the membrane surface (Koros and Chern, 1987; Koros and Pinnau, 1994). Thus, with higher shear and higher orientation in the polymeric matrix, the effect of the chain mobility restriction will cause size-dependent reduction in mobility of gases, leading to a higher selectivity. However, it must be noted that, due to membrane surface defects, the selectivities of these uncoated fibers expressed by the solution diffusion mechanism are still well below the intrinsic selectivity of the polymer.

As expected, the selectivities of these PES hollow fibers increase dramatically after being coated with high-permeability silicone rubber because the defects on the membrane outer surface that undermine the intrinsic selectivity of the membrane are caulked. In addition, it is worth noting that the selectivities of these hollow fibers regardless of low or high shear for most of our studied gas pairs either are very close to or far exceed the intrinsic selectivity of a homogeneous dense PES membrane, as illustrated in Table 9.

The most striking one is the selectivity of H_2/N_2 for fibers spun with high shear rate; it is 4-fold of the PES intrinsic value (292−307 vs 73.7). This high selectivity is due to the fact that hydrogen has not only a linear but also a smaller molecule which can diffuse through the highly oriented outer skin faster than N_2.

3. Thermal and Mechanical Properties. Thermomechanical analysis was used in order to confirm our hypothesis that the significant improvement in gas selectivity is due to the enhanced molecular orientation induced by shear stress during the hollow fiber spinning. Table 10 illustrates that the calculated CTE of these hollow fibers decreases with an increase in shear induced. This result is in agreement with the previous work in which an increase in the draw ratio or molecular

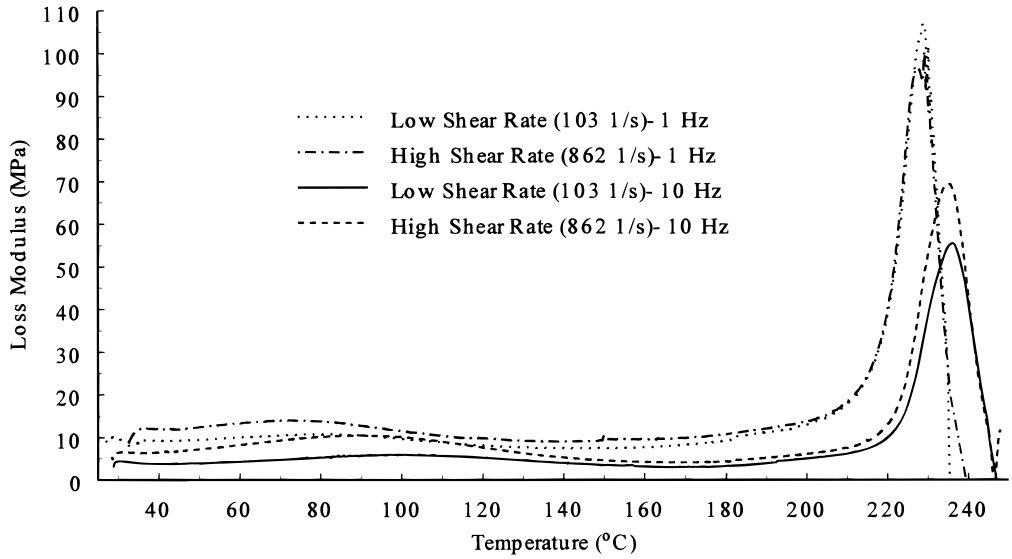

Figure 6. Loss modulus vs temperature as a function of shear rate and frequency measured by DMA.

Table 10. T_g and CTE as a Function of Shear Rate (TMA)

calcd shear rate (1/s)	T_g (°C)	CTE (μm/m °C)
103	213.8	83.5
862	213.5	75

orientation results in a decrease in CTE (Turi, 1981). Figure 6 illustrates the lost modulus of DMA curves of hollow fibers spun at low shear and high shear as a function of temperature at a frequency of 10 Hz and indicates the β transition of these membranes to be around 91−109 °C for 10 Hz. The secondary or β transition of the high-sheared membranes is more significant than that of the low-sheared membranes. This is due to the fact that β transition corresponds to the motion of molecular segments (side groups, e.g., carbonyl group). A higher orientated molecular chain tends to have a greater loss modulus during molecular chain relaxation and rearrangement because the former possesses a higher excess energy that dissipates as heat when it is free to move.

Future Work

Although we have demonstrated the importance of shear effect on the morphology and separation performance of wet-spun hollow fibers, there are many other interesting topics worthwhile to be further explored. For example, what is the minimum shear rate or stress to induce molecular orientation that may result in a significant impact on the membrane separation performance? What is the effect of Deborah number (ratio of the characteristic time for the spinning solution to the characteristic time for the spinning system) on fiber formation? What is the critical $L/\Delta D$ ratio to enhance shear effect on fiber formation? What is the separation performance of CO_2/CH_4 of the highly shear-induced hollow fibers? Does bore fluid induce hoop stress upon the outer skin of the nascent fiber and therefore enhance membrane performance? All of these have to be answered by membrane scientists.

Conclusions

By using the wet phase inversion process, water as the external coagulant, and 80/20 NMP/H_2O as the bore fluid, we have determined the effect of shear stress and shear experience within a spinneret during hollow fiber spinning on membrane morphology, gas separation performance, and thermal and mechanical properties. We observed a difference in morphology among hollow fibers spun with different shear levels. Threadlike fibers were found on the inner skin of high-sheared membranes due to the shear deformation of polymeric agglomerates. We could not identify the nodular structure that has been observed previously in the as-cast flat membranes or at the outer skin of the hollow fibers spun from the spinneret with a short $L/\Delta D$ ratio. This result suggests that the fully developed high shear stress within the spinneret may alter the thermodynamics of polymeric solution and thus nodular formation.

Most of the selectivities of gas pairs under study exceed the intrinsic selectivity of the PES polymer. For example, the selectivity of H_2/N_2 for fibers spun from the newly developed spinneret with high shear is 4-fold of the intrinsic PES value (292−307 vs 73.7). The thermomechanical properties of the hollow fibers in terms of the coefficient of thermal expansion (CTE) are enhanced by higher shear during spinning due to a greater molecular orientation. In the same manner, the loss modulus or heat dissipation of the high-sheared membranes is higher than that of the low-sheared membranes under a dynamic environment.

Acknowledgment

The authors thank Dr. S. J. Shilton of University of Strathclyde for his useful comments and the National University of Singapore (NUS) (Research Fund No. RP960609A) and ET Enterprise in NUS (Research Fund Nos. RP 960609A and RP 3602037) for funding this project. Special thanks are due Drs. J. J. Shieh and Z. Xu, Mr. S. L. Liu, and Ms. K. Ma from the Department of Chemical Engineering, Mr. K. S. Ng and Mrs. C. M. Ho from the Department of Electrical Engineering, Mr. S. K. Tung from the Department of Mechanical Engineering, and Prof. J. Phang at Image Transform Limited Inc. for the use of their SEM microscopes, Mr. K. P. Ng for the help in fabrication and machinery, Mdm K. L. Leong for assistance, and the Institute of Materials

Research and Engineering of Singapore for use of their equipment.

Literature Cited

Aptel, P.; Cabasso, I. Development of a new asymmetric alloy membrane for water desalination. *Desalination* **1981**, *36*, 25.

Aptel, P.; Abidine, N.; Ivaldi, F.; Lafaille, J. P. Polysulfone hollow fibres—effect of spinning conditions on ultrafiltration properties. *J. Membr. Sci.* **1985**, *22*, 199.

Bird, R. B.; Armstrong, R. C.; Hassager, O. Dynamics of polymeric liquids. *Fluid mechanics*, 2nd ed.; John Wiley and Sons: New York, 1987; Vol. 1.

Borneman, Z.; van't Hoff, J. A.; Smolders, C. A.; van Veen, H. M. Hollow fibre gas separation membranes: structure and properties. *4th BOC Priestly Conference*; Royal Society of Chemistry: London, 1986; p 145.

Chung, T. S. The Limitations of Using Flory−Huggins Equation for the States of Solutions During Asymmetric Hollow Fiber Formation. *J. Membr. Sci.* **1997**, *126*, 19.

Chung, T. S.; Kafchinski, E. R. The Effects of Spinning Conditions on Asymmetric 6FDA/6FDAM Polyimide Hollow Fibers For Air-Separation. *J. Appl. Polym. Sci.* **1997**, *65*, 1555.

Chung, T. S.; Teoh, S. K. Breaking The Limitation of Composition Change During Isothermal Mass-Transfer Processes at the Spinodal. *J. Membr. Sci.* **1997**, *130*, 141.

Chung, T. S.; Teoh, S. K.; Hu, X. Formation of ultrathin high-performance polyethersulfone hollow fibre membranes. *J. Membr. Sci.* **1998**, *133*, 161.

Criado-Sancho, M.; Jou, D.; Casas-Vazquez, J. Definition of nonequilibrium chemical potential: phase separation of polymers in shear flow. *Macromolecules* **1991**, *24*, 2834.

Criado-Sancho, M.; Casas-Vazquez, J.; Jou, D. Hydrodynamic interaction and the shear induced shift of the critical point in polymer solutions. *Polymer* **1995**, *21*, 4107.

Crochet, M. J.; Davies, A. R.; Walters, K. *Numerical Simulation of Non-Newtonian Flow*; Elsevier: New York, 1984; p 236.

East, G. C.; McIntyre, J. E.; Rogers, V.; Senn, S. C. Production of porous hollow polysulphone fibres for gas separation. *4th BOC Priestly Conference*; Royal Society of Chemistry: London, 1986; p 130.

El-hibri, M. J.; Paul, D. R. Effects of uniaxial drawing and heat-treatment on gas sorption and transport in PVC. *J. Appl. Polym. Sci.* **1985**, *30*, 3649.

Fredrickson, A.; Bird, R. B. Non-Newtonian flow in annuli. *Ind. Eng. Chem.*, **1958**, *50*, 347.

Ismail, A. F.; Shilton, S. J.; Dunkin, I. R.; Gallivan, S. L. Direct measurement of rheologically induced molecular orientation in gas separation hollow fibre membranes and effects on selectivity. *J. Membr. Sci.* **1997**, *126*, 133.

Kesting, R. E.; Fritzsche, A. K. *Polymeric gas separation membranes*; John Wiley and Sons: New York, 1993.

Koros, W. J.; Chern, R. T. Separation of gaseous mixtures using polymer membranes. *Handbook of separation process technology*; Rosseau, R., Ed.; John Wiley and Sons: New York, 1987; Chapter 20, p 862.

Koros, W. J.; Pinnau, I. Membrane formation for gas separation processes. *Polymeric Gas Separation Membranes*; Paul, D. R., Yampol'skii, Y. P. Eds.; CRC Press: Boca Raton, FL, 1994; Chapter 5, p 209.

Loeb, S.; Sourirajan, S. Sea water demineralization by means of an osmotic membrane. *Adv. Chem. Ser.* **1963**, *38*, 117.

Mark, J. E.; Eisenberg, A.; Graessley, W. W.; Mandelkern, L.; Koenig, J. L. *Physical properties of polymers*; American Chemical Society: Washington, DC, 1984.

Matsuura, T. Synthetic membranes and membrane separation process. CRC Press: Boca Raton, FL, 1994; Chapter 5.

McHugh, A. J.; Miller, D. C. The dynamics of diffusion and gel growth during nonsolvent-induced phase inversion of polyethersulfone. *J. Membr. Sci.* 1995, *105*, 121.

Murayama, T. Dynamic mechanical properties. *Encyclopedia of polymer science and engineering*; John Wiley & Sons: New York, 1985−1990; Vol. 5, p 299.

Paul, D. R. Spin orientation during acrylic fibre formation. *J. Appl. Polym. Sci.* **1969**, *13*, 817.

Pearson, J. R. A. *Mechanics of polymer processing*; Elsevier Applied Science Publishers: London, 1985; p 190.

Pinnau, I.; Koros, W. J. Relationship between substructure resistance and gas separation properties of defect-free integrally skinned asymmetric membranes. *Ind. Eng. Chem. Res.* **1991**, *20*, 1837.

Puri, P. S. Fabrication of hollow fibre gas separation membranes. *Gas Sep. Purif.* **1990**, *4*, 29.

Shilton, S. J. Flow profile induced in spinneret during hollow fiber membrane spinning. *J. Appl. Polym. Sci.* **1997**, *65*, 1359.

Shilton, S. J.; Bell, G.; Ferguson, J. The rheology of fibre spinning and the properties of hollow fibre membranes for gas separation. *Polymer* **1994**, *35*, 5327.

Shilton, S. J.; Bell, G.; Ferguson, J. The deduction of fine structural details of gas separation hollow fibre membranes using resistance modelling of gas permeation. *Polymer* **1996**, *37*, 485.

Tadmor, Z.; Gogos, C. G. *Principles of polymer processing*; John Wiley and Sons: New York, 1979; p 543.

Turi, E. A. *Thermal Characterisation of Polymeric Materials*; Corporate Research and Development, Allied Corp.: Morristown, NJ, 1981.

Wang, D. Polyethersulfone hollow fibre gas separation membranes prepared from solvent systems containing nonsolvent additives. Ph.D. Dissertation, National University of Singapore, 1996.

Wienk, I. M.; Boom, R. M.; Beerlage, M. A. M.; Bulte, A. M. W.; Smolders, C. A.; Strathmann, H. Recent advances in the formation of phase inversion membranes made from amorphous or semicrystalline polymers. *J. Membr. Sci.* **1996**, *113*, 361.

Wolf, B. A. Thermodynamic theory of flowing polymer solutions and its applications to phase separation. *Macromolecules* **1984**, *17*, 615.

Yang, M.; Chou, M. Effect of post-drawing on the mechanical and mass transfer properties of polyacrylonitrile hollow fibre membranes. *J. Membr. Sci.* **1996**, *116*, 279.

Received for review April 1, 1998
Revised manuscript received June 17, 1998
Accepted June 19, 1998

IE9802111